

Title: Phenology and diversity in Zambia

Authors: Godlee, J. L.¹,

¹: School of GeoSciences, University of Edinburgh, Edinburgh, United Kingdom

Corresponding author:

John L. Godlee

johngodlee@gmail.com

School of GeoSciences, University of Edinburgh, Edinburgh, United Kingdom

Acknowledgements

Author contribution statement

Data accessibility statement

Abstract

1 Introduction

The seasonal timing of tree leaf production in dry deciduous savannas directly influences ecosystem processes and structure (). Leaf Area Index (LAI), leaf area per unit ground area, is tightly coupled with photosynthetic activity and therefore Gross Primary Productivity (GPP) (). Directional shifts in GPP influence the accumulation rate of woody biomass, and affect the delicate balance between tree and grass co-occurrence in these ecosystems (), with potential consequences for transition between closed-canopy forest and open savanna. From a conservation perspective, deciduous savannas with a longer growth period support a greater diversity and abundance of wildlife, particularly bird species but also browsing mammals (). Extreme weather patterns as a result of climate change are leading to shorter but more intense leaf production cycles in these ecosystems which exist at the precipice of their climatic envelope, with severe negative consequences for biodiversity (). Understanding the determinants of seasonal patterns of tree leaf production (land-surface phenology) in dry deciduous savannas can provide valuable information on spatial variation in vulnerability to climate change, and help to model their contribution to land surface models under climate change.

Previous studies have shown that diurnal temperature variation and precipitation are the primary determinants of tree phenological activity in water-limited savannas (). At regional spatial scales, savanna phenological activity can be predicted well using only climatic factors and light environment (Adole, Dash, and Atkinson, 2018), but local variation exists in leaf production cycles which cannot be attributed solely to abiotic environment (). It has been repeatedly suggested that information on biotic environment play a larger role in predicting land-surface phenology (), but implementation is most often limited to coarse ecoregions or functional vegetation types (), which lack the fine-scale resolution which can now be paired with state-of-the-art earth observation data.

Tree species vary in their life history strategy regarding the timing of leaf production (). More conservative species (i.e. slower growing, robust leaves, denser wood) tend to initiate leaf production (green-up) before rainfall has commenced, and persist after the rainy season has finished, despite having lower overall GPP, while more resource acquisitive species and juvenile individuals tend to green-up during the rainy season, and create a dense leaf-flush during the mid-season peak of growth (). It has been suggested that this variation in leaf phenological activity between species is one aspect by which increased tree species richness causes an increase in ecosystem-level productivity in deciduous savannas (). Building on research linking biodiversity and ecosystem function, one might expect that an ecosystem with a greater diversity of tree species might be better able to maintain consistent leaf coverage for a longer period over the year, as species vary in their optimal growing conditions due to niche complementarity, whereby coexisting species vary in their occupation of niche space due to competitive exclusion ().

In the water-limited savannas such as those found in large areas of southern Africa (), the ability of conservative tree species to maintain consistent leaf coverage in the upper canopy strata over the growing season, but particularly at the start and end of the growing season, may provide facilitative effects to other tree species and juveniles occupying lower canopy strata that are less

well-adapted to moisture-limiting conditions, but are more productive, by providing shade and influencing below ground water availability through hydraulic lift ().

Variation in tree species composition, as well as species richness, is also expected to have an effect on savanna phenology in southern Africa. Savannas of a number of different types (species composition and structure) are found across southern Africa, but these are often poorly differentiated in regional-scale phenological studies (), resulting in a dearth of information on the phenological behaviour of different woodlands. As our ability to remotely sense tree species composition improves, it allows us to create more tailored models of the carbon cycle which incorporate not only climatic factors, but also biotic factors which govern productivity. We therefore need to understand how species composition and biodiversity metrics affect land-surface phenology.

In the deciduous woodlands of Zambia, a highly pronounced single wet-dry season annual oscillation is observed across the majority of land area, with local exceptions in some mountainous areas (). Variation in leaf phenological activity across the country has a large influence on annual gross primary productivity. Using Zambia as a case study, we can expect similar response from deciduous woodlands across southern Africa, with important consequences for the global carbon cycle ().

While cumulative leaf production across the growing season may be the most important aspect of leaf phenology for GPP, other phenological metrics may be more important for ecosystem function and habitat provision for wildlife. Periods of green-up and senescence which bookend the growing season are key times for invertebrate reproduction (), soil biotic activity () and herbivore browsing activity (). Pre-rainy season green-up in water-limited savannas provides a valuable source of moisture and nutrients before the rainy season, and can moderate the understorey microclimate, increasing humidity, reducing UV exposure, and moderating diurnal oscillations in temperature, reducing ecophysiological stress which can lead to mortality during the dry season. An increase in the time between leading tree growth and the onset of seasonal rains provides a buffer to stressful dry season climatic conditions and wildlife activity. A slower rate of green-up caused by tree species greening at different times provides an extended period of bud-burst, thus maintaining the important food source of nutrient rich young leaves for longer ().

In this study we contend that, across Zambian deciduous savannas, tree species diversity and composition influence three key measurable aspects of the tree phenological cycle: (1) the rates of greening and senescence at the start and end of the seasonal growth phase, (2) the overall length of the growth period, and (3) the lag time between green-up/senescence and the start/end of the rainy season. It is hypothesised that: (H₁) due to variation among species in minimum viable water availability for growth, plots with greater tree species richness will exhibit slower rates of greening and senescence as different species green-up and senesce at different times. We expect that: (H₂) in plots with greater species richness the start of the growing season will occur earlier in respect to the onset of rain due to an increased likelihood of containing a species which can green-up early, facilitating other species to initiate the growing season. We hypothesise that: (H₃) plots with greater species richness will exhibit a longer growth period and greater cumulative green-ness over the course of the growth period, due to a higher resilience to variation in water availability, acting as a buffer to ecosystem-level productivity. Finally, we hypothesise that: (H₄) irrespective of species diversity, variation in tree species composition and vegetation type will

83 cause variation in the phenological metrics outlined above.

84 2 Materials and methods

85 2.1 Data collection

86 We used plot-level data on tree species diversity across 607 sites from the Zambian Integrated
87 Land Use Assessment Phase II (ILUA-II), conducted in 2014 (Mukosha and Siampale, 2009; Pel-
88 letier et al., 2018). Each site consisted of four 20x50 m (0.2 ha) plots positioned in a square around
89 a central point, with a distance of 500 m between each plot (Figure 2). The original census con-
90 tained 993 sites, which was filtered in order to define study bounds and to ensure data quality.
91 Only sites with ≥ 50 stems ha^{-1} ≥ 10 cm DBH (Diameter at Breast Height) were included in the
92 analysis, to ensure all sites represented woody savanna rather than ‘grassy savanna’, which is con-
93 sidered a separate biome with very different species composition and ecosystem processes govern-
94 ing phenology (Parr et al., 2014). Sites in Mopane woodland were removed by filtering sites with
95 greater than 50% of individuals belonging to *Colophospermum mopane*, preserving only plots with
96 Zambesian tree savanna / woodland. To eliminate compositional outliers, plots with fewer than
97 five species with more than one individual were excluded. Plots dominated by non-native tree
98 species ($\geq 50\%$ of individuals), e.g. *Pinus* spp. and *Eucalyptus* spp. were also excluded, as these
99 species may exhibit non-seasonal patterns of leaf production ().

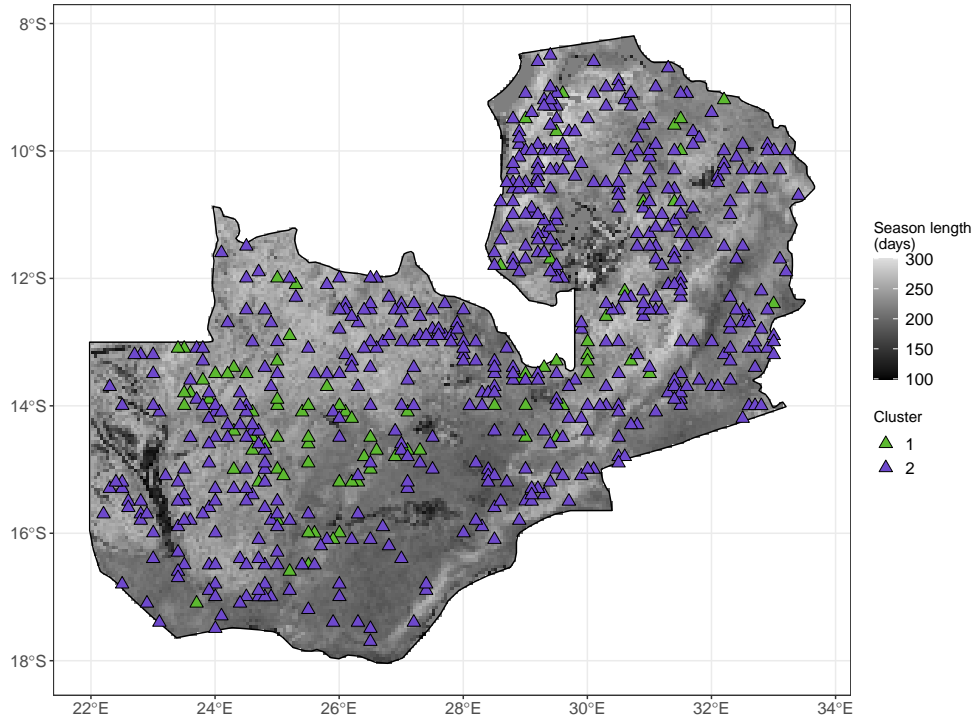


Figure 1: Distribution of study sites within Zambia as triangles, each consisting of four plots. Sites are coloured according to vegetation compositional cluster as identified by Ward's clustering algorithm on euclidean distance of plots in the first two axes of NSCA ordination space. Zambia is shaded according to growing season length as estimated by the MODIS VIPPHEN-EVI2 product, at 0.05 degrees spatial resolution (Didan and Barreto, 2016).

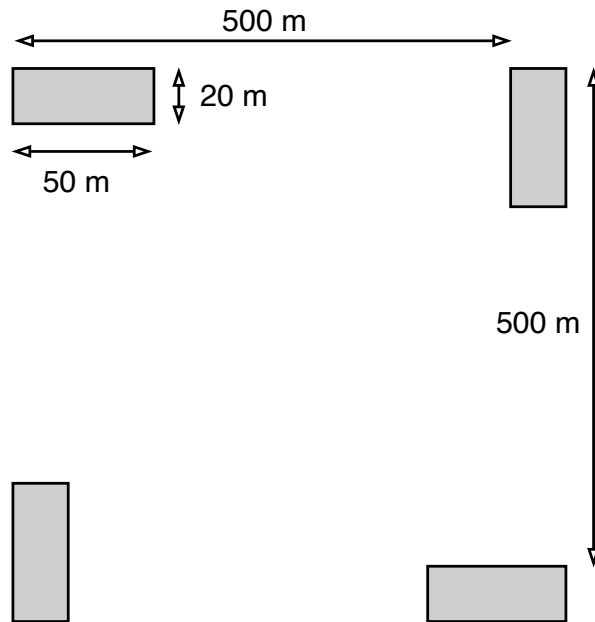


Figure 2: Schematic diagram of plot layout within a site. Each 20x50 m (0.2 ha) plot is shaded grey. The site centre is denoted by a circle. Note that the plot dimensions are not to scale.

100 Within each plot, the species of all trees with at least one stem ≥ 10 cm DBH were recorded. Plot
 101 data was aggregated to the site level for analyses to avoid pseudo-replication caused by the more
 102 spatially coarse phenology data. Tree species composition varied little among the four plots within
 103 a site, and were treated as representative of the woodland in the local area. Using the Bray-Curtis
 104 dissimilarity index of species abundance data, we calculated that the mean pairwise compositional
 105 distance between plots within a site was lower than the mean compositional distance across all
 106 pairs of plots in 92.7% of cases.

107 To quantify phenology at each site, we used the MODIS MOD13Q1 satellite data product at 250
 108 m resolution (Didan, 2015). The MOD13Q1 product provides an Enhanced Vegetation Index (EVI)
 109 time series at 16 day intervals. EVI is widely used as a measure of vegetation growth, as an im-
 110 provement to NDVI (Normalised Differential Vegetation Index), which tends to saturate at higher
 111 values. EVI is well-correlated with gross primary productivity and so can act as a suitable proxy
 112 (). We used all scenes from January 2015 to August 2020 with less than 20% cloud cover covering
 113 the study area. All sites were determined to have a single annual growth season according to the
 114 MODIS VIPPHEN product (), which assigns pixels (0.05° , 5.55 km at equator) up to three growth
 115 seasons per year. We stacked yearly data between 2015 and 2020 and fit a General Additive Model
 116 (GAM) to produce an average EVI curve. We estimated the start and end of the growing season
 117 using first derivatives of the GAM. We identified the start of the growing season as the first day
 118 where the model slope exceeds a slope of 2, which is maintained or exceeded for 10 or more days.
 119 Similarly, we defined the end of the growing season as the end of the latest 10 day period where
 120 the model slope is below -2. We estimated the length of the growing season as the number of days
 121 between the start and end of the growing season. We estimated the green-up rate as the slope of
 122 a linear model across EVI values between the start of the growing season and the point at which
 123 the slope of increase reduces below 2. Similarly the senescence rate was estimated as the slope of a
 124 linear model between the point where the slope of decrease fell below -2 and the end of the grow-
 125 ing season Figure 3. We validated our calculations of cumulative EVI, mean annual EVI, growing
 126 season length, season start date, season end date, green-up rate and senescence rate with calcu-
 127 lations made by the MODIS VIPPHEN product with linear models comparing the two datasets
 128 across our study sites (Figure S1, Table S1). Sites where our calculation of a phenological metric
 129 was drastically different to the MODIS VIPPHEN estimate were excluded, under the assumption
 130 that our algorithm had failed to capture the true value. This removed 175 sites.

131 Precipitation data was gathered using the “GPM IMERG Final Precipitation L3 1 day V06” dataset,
 132 which has a pixel size of 0.1° (11.1 km at the equator) (**GPM**), between 2015 and 2020. Daily to-
 133 tal precipitation was separated into two periods: precipitation during the growing season (growing
 134 season precipitation), and precipitation in the 90 day period before the onset of the growing sea-
 135 son (dry season precipitation). Similar to estimation of the growing season, the rainy season was
 136 defined using the first derivative of a GAM to create a curve for each site using stacked yearly pre-
 137 cipitation data. The slope coefficient used to identify the start and end of the rainy season was
 138 0.06. Mean diurnal temperature range (Diurnal δT) was calculated as the mean of monthly tem-
 139 perature range from the WorldClim database, using the BioClim variables, with a pixel size of 30
 140 arc seconds (926 m at the equator) (Fick and Hijmans, 2017). averaged across all years of avail-
 141 able data (1970-2000).

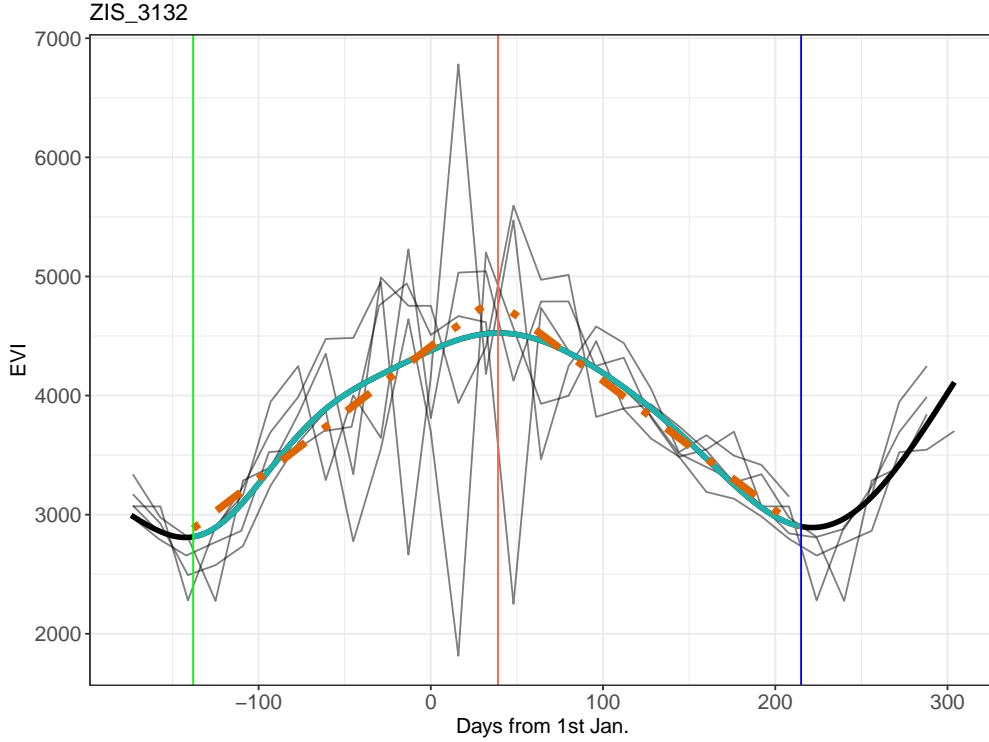


Figure 3: Example EVI time series, demonstrating the metrics derived from it. Thin black lines show the raw EVI time series, with one line for each annual growth season. The thick black line shows the GAM fit. The thin blue lines show the minima which bound the growing season. The red line shows the maximum EVI value reached within the growing season. The shaded cyan area of the GAM fit shows the growing season, as defined by the first derivative of the GAM curve. The two orange dashed lines are linear regressions predicting the green-up rate and senescence rate at the start and end of the growing season, respectively. Note that while the raw EVI time series fluctuate greatly around the middle of the growing season, mostly due to cloud cover, the GAM fit effectively smooths this variation to estimate the average EVI during the mid-season period.

2.2 Data analysis

To measure variation in tree species composition we used a combination of Non-symmetric Correspondence Analysis (NSCA) and agglomerative hierarchical clustering on species abundance data (Kreft2010; Fayolle2014), and was performed using the `ade4` R package (Dray and Dufour, 2007). To guard against sensitivity to rare individuals, which can preclude meaningful cluster delineation across such a large species compositional range, we restricted the NSCA to species with greater than five records, and to sites with fewer than five species (). We used Ward’s algorithm to define clusters (Murtagh2014), based on the euclidean distance of sites in NSCA ordination space. We determined the optimal number of clusters by maximising the mean silhouette width among clusters (Rousseeuw1987) Figure S2. Vegetation type clusters were used later as interaction terms in linear models. We described the vegetation types represented by each of the clusters using a Dufrene-Legendre indicator species analysis (Dufrene1997).

We specified multivariate linear models to assess the role of tree species diversity on each of the

chosen phenological metrics. We defined tree species diversity using both species richness and abundance evenness as separate independent variables. Abundance evenness was calculated as the Shannon Equitability index ($E_{H'}$) (Smith1996) was calculated as the ratio of the Shannon diversity index to the natural log of species richness. We defined a maximal model structure including tree species richness, abundance evenness, the interaction of species richness and vegetation type, and climatic variables shown by previous studies to strongly influence phenology. The quality of the maximal model was compared to models with different subsets of independent variables using the model log likelihood, AIC (Akaike Information Criteria), BIC (Bayesian Information Criteria), and adjusted R^2 values for each model. For each phenological metric, the best model according to the model quality statistics is reported in the results. Where two similar models were within 2 AIC points of each other, the model with fewer terms was chosen as the best model, to maximise model parsimony. All models were fitted using Maximum Likelihood (ML) to allow comparison of models (). The best model was subsequently re-fitted using Restricted Maximum Likelihood for model effect estimation (REML). Independent variables in each model were transformed to achieve normality where necessary and standardised to Z-scores prior to modelling to allow comparison of slope coefficients within a given model.

We used the **ggeffects** package to estimate the marginal means of the interaction effect of species richness and vegetation type, to investigate vegetation type specific effects on each phenological metric (**ggeffects**). Estimated marginal means entails generating model predictions across values of a focal variable, in this case species richness, while holding non-focal variables constant. All statistical analyses were conducted in R version 4.0.2 (R Core Team, 2020).

3 Results

Model selection showed that richness and evenness are important determinants of each of the chosen phenological metrics, across vegetation types. Species richness featured in all models, though was not significant in cumulative EVI or senescence rate, while evenness was included in models for cumulative EVI and season length only Figure 4.

NSCA used 4 axes, which accounted for 11.7% of the variance according to eigenvalue decay. 2 were identified during clustering. Pairwise Wilcoxon Signed Rank Tests showed that clusters were significantly different in species composition ($p < 0.05$).

In models for green-up lag and senescence lag, species richness had consistent effects on the phenological response to rainy season onset and decline. Species richness caused green-up to occur increasingly earlier with respect to the rainy season onset, while richness caused senescence onset to occur later after the end of the rainy season.

Against expectations, tree species evenness had a negative effect on cumulative EVI, and richness had a negligible, non-significant effect. Wet season precipitation had a positive effect and diurnal temperature range had a negative effect, as expected. Despite this, species richness had a significant positive effect on season length. It is striking that richness and evenness have contrasting effects on season length.

All models were of better quality than models which included only climatic variables Table 2. The

phenological metrics best predicted were green-up lag and season length, where models explained 25% and 24% of the variance in these variables, respectively. Senescence rate and senescence lag were the least well predicted phenological metrics, with the best model explaining 5% and 10% of their variance, respectively.

The slope of the relationship between species richness and phenological metrics varied among vegetation types, but largely maintained the same direction Figure 5. Models predicting green-up and senescence lag had the tightest confidence intervals among vegetation type marginal effects.

The hierarchical clustering analysis demonstrated that there was some degree of spatial structure to the vegetation types. Sites classified as within cluster 3 were found predominantly in the south and southwest of the country, while sites in cluster 2 were found predominantly in the north. Cluster 1 sites were restricted mostly to the centre and northwest of the country Figure 1.

Cluster	Species	Indicator value
1	<i>Julbernardia paniculata</i>	0.876
	<i>Psuedolachnostylis maprouneifolia</i>	0.416
	<i>Pericopsis angolensis</i>	0.375
2	<i>Brachystegia spiciformis</i>	0.450
	<i>Pterocarpus angolensis</i>	0.399
	<i>Diplorhynchus condylocarpon</i>	0.388

Table 1: Legendre indicator species analysis for the four vegetation type clusters identified by the PAM algorithm.

Response	δ AIC	δ BIC	R^2_{adj}	δ logLik
Cumulative EVI	-1.9	-15.1	0.10	-2.04
Season length	13.4	4.6	0.13	-8.69
Green-up rate	-1.3	-10.1	0.08	-1.37
Senescence rate	1.0	-7.8	0.06	-2.50
Green-up lag	59.2	46.0	0.23	-32.59
Senescence lag	35.5	26.7	0.08	-19.74

Table 2: Model fit statistics for each phenological metric.

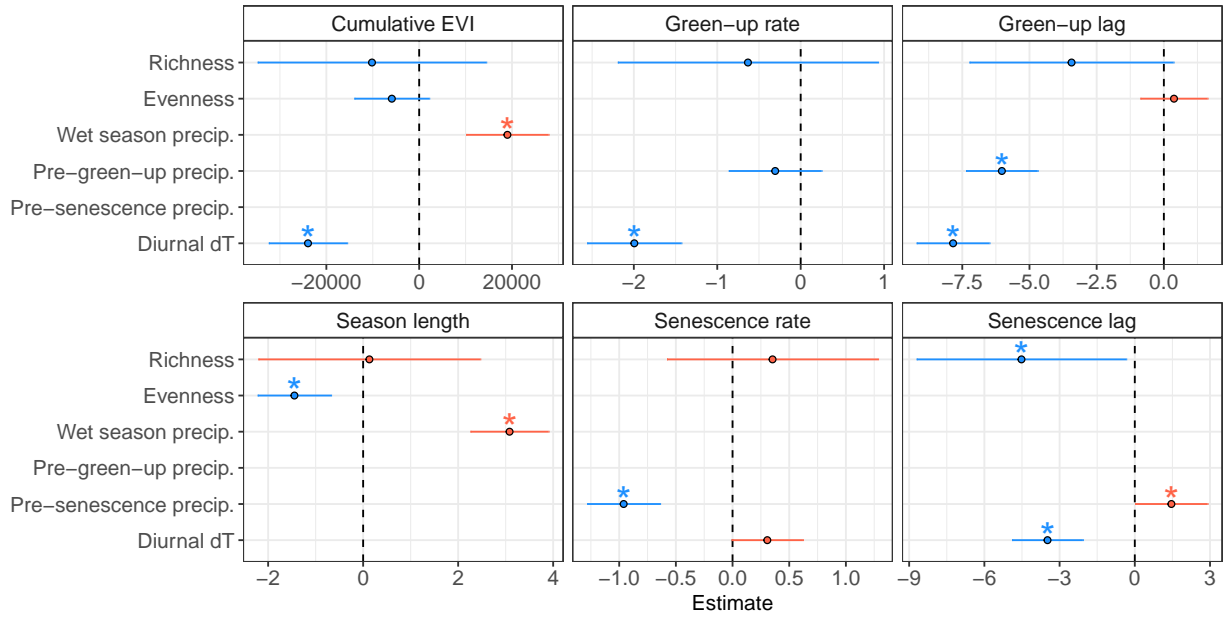


Figure 4: Standardized slope coefficients for each best model of a phenological metric. Slope estimates are ± 1 standard error. Slope estimates where the interval (standard error) does not overlap zero are considered to be significant effects.

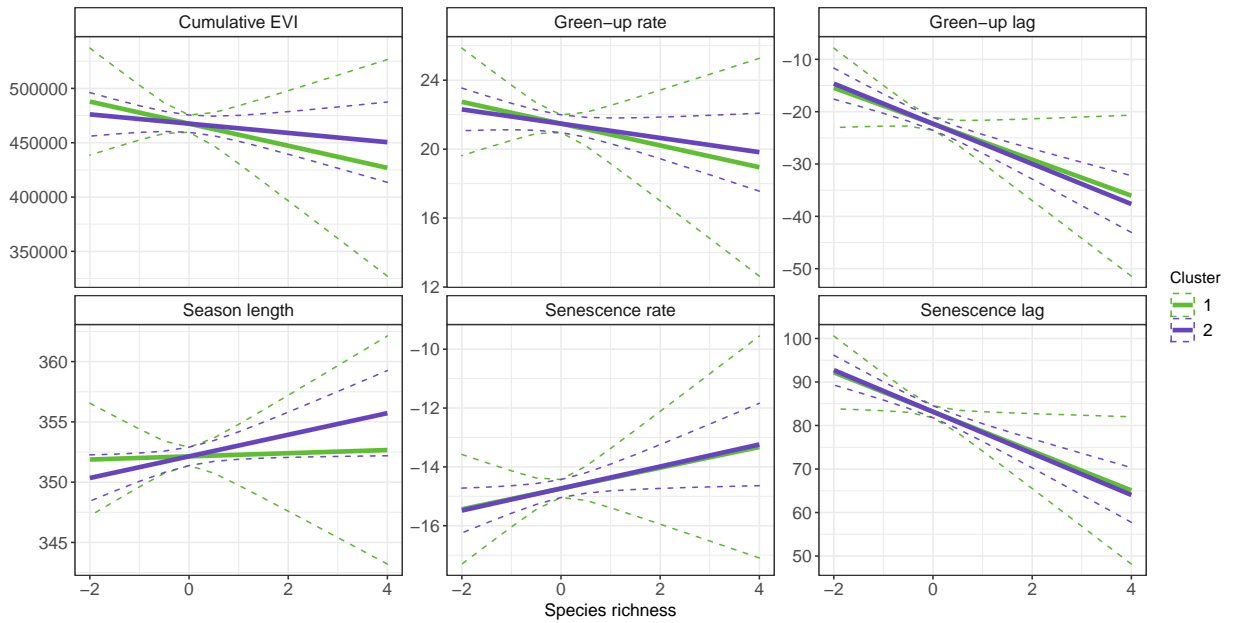


Figure 5: Marginal effects of tree species richness on each of the phenological metrics, for each vegetation type, using the best model for each phenological metric.

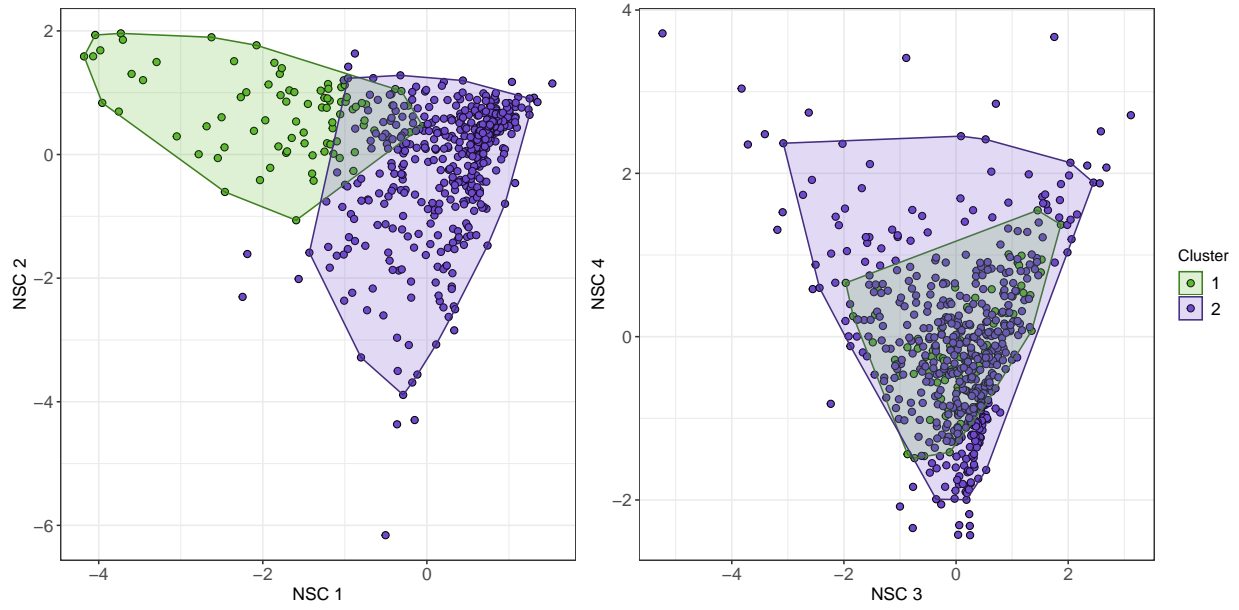


Figure 6: Plot scores of the (A) first and second, and (B) third and fourth axes of the Non-Symmetric Correspondence Analysis of tree species composition. Points are coloured according to clusters defined by Ward's algorithm on euclidean distances of the NSCA ordination axes, along with a convex hull encompassing 95% of the points in each cluster.

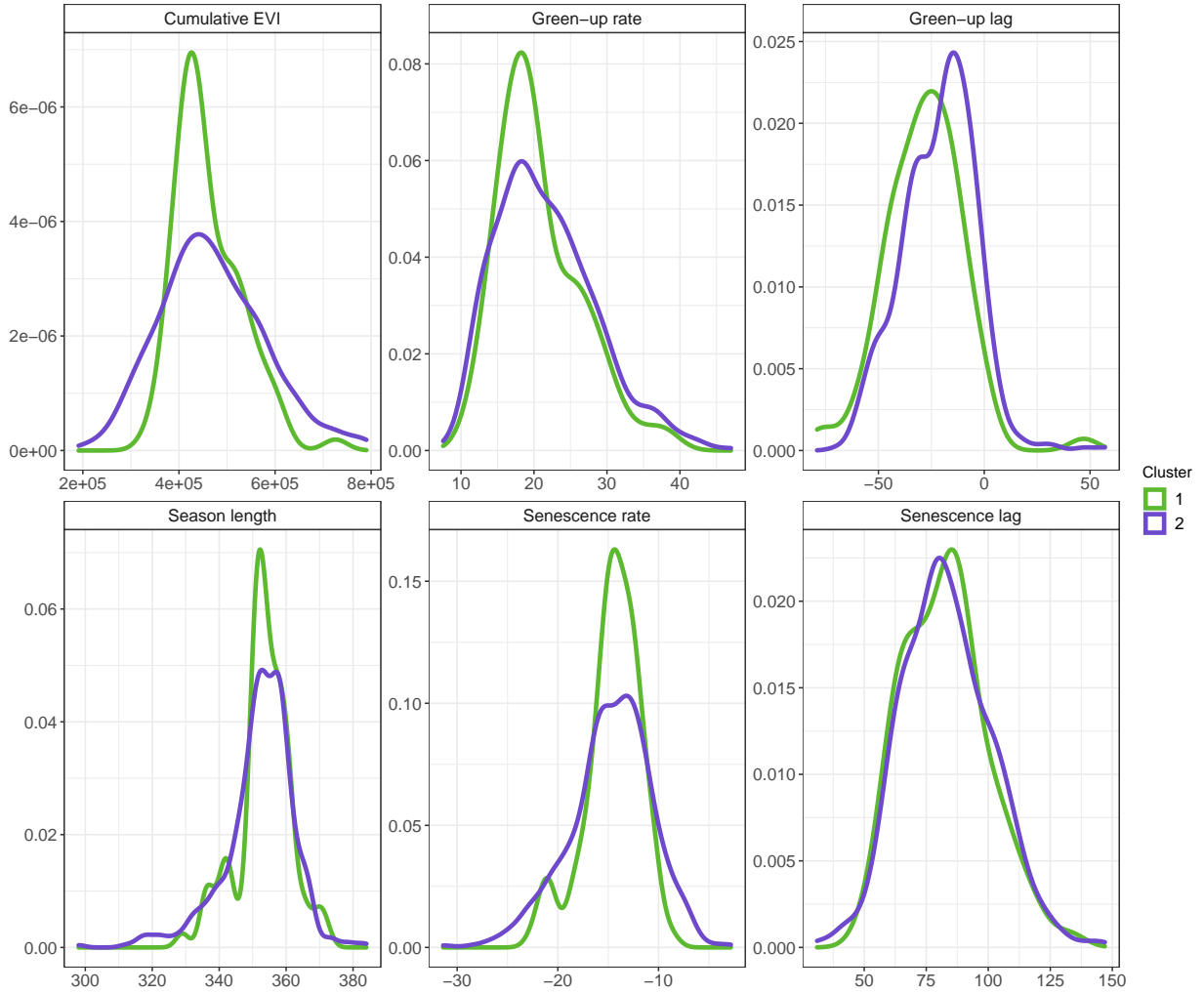


Figure 7

4 Discussion

The ability for us now nearing to be able to remotely sense tree species diversity allows us to make more tailored models of the carbon cycle which incorporate not only climatic factors, but also biotic factors which govern productivity. We therefore need to understand how species composition and biodiversity metrics affect land-surface phenology.

It's possible that the reason we couldn't predict season length well is that there is very little variation between sites. Notably, only cluster three deviates from the density distribution of the other two clusters, with more sites at the lower end of the distribution. Cluster 3 also differed in significantly in senescence rate from the other two clusters, with many more plots showing a very steep senescence rate. Interestingly, Cluster three had wider variation in cumulative EVI than the other clusters and this is reflected in the marginal effects of species richness on these phenological metrics. Species richness had a greater effect on cumulative EVI than the other two clusters, and led to a steeper senescence rate.. **WHYTHO?**

Important to note that the EVI measurements don't refer only to trees, they are the whole ecosystem. But I don't think that makes the results less important or valid.

5 Conclusion

References

- Adole, Tracy, Jadunandan Dash, and Peter M. Atkinson (2018). “Large-scale prerain vegetation green-up across Africa”. In: *Global Change Biology* 24.9, pp. 4054–4068. DOI: 10.1111/gcb.14310.
- Didan, L. (2015). *MOD13Q1 MODIS/Terra Vegetation Indices 16-Day L3 Global 250m SIN Grid V006 [Data set]*. NASA EOSDIS Land Processes DAAC. DOI: 10.5067/MODIS/MOD13Q1.006. (Visited on 08/05/2020).
- Didan, L. and A. Barreto (2016). *NASA MEaSUREs Vegetation Index and Phenology (VIP) Phenology EVI2 Yearly Global 0.05Deg CMG [Data set]*. NASA EOSDIS Land Processes DAAC. DOI: 10.5067/MEaSUREs/VIP/VIPPHEN_EVI2.004. (Visited on 08/05/2020).
- Dray, Stéphane and Anne-Béatrice Dufour (2007). “The ade4 Package: Implementing the Duality Diagram for Ecologists”. In: *Journal of Statistical Software* 22.4, pp. 1–20. DOI: 10.18637/jss.v022.i04.
- Fick, S. E. and R. J. Hijmans (2017). “WorldClim 2: New 1-km spatial resolution climate surfaces for global land areas”. In: *International Journal of Climatology* 37.12, pp. 4302–4315. DOI: <http://dx.doi.org/10.1002/joc.5086>.
- Mukosha, J and A Siampale (2009). *Integrated land use assessment Zambia 2005–2008*. Lusaka, Zambia: Ministry of Tourism, Environment et al.
- Parr, C. L. et al. (2014). “Tropical grassy biomes: misunderstood, neglected, and under threat”. In: *Trends in Ecology and Evolution* 29, pp. 205–213. DOI: 10.1016/j.tree.2014.02.004.
- Pelletier, J. et al. (2018). “Carbon sink despite large deforestation in African tropical dry forests (miombo woodlands)”. In: *Environmental Research Letters* 13, p. 094017. DOI: 10.1088/1748-9326/aadc9a.
- R Core Team (2020). *R: A Language and Environment for Statistical Computing*. R Foundation for Statistical Computing, Vienna, Austria. URL: <https://www.R-project.org/>.

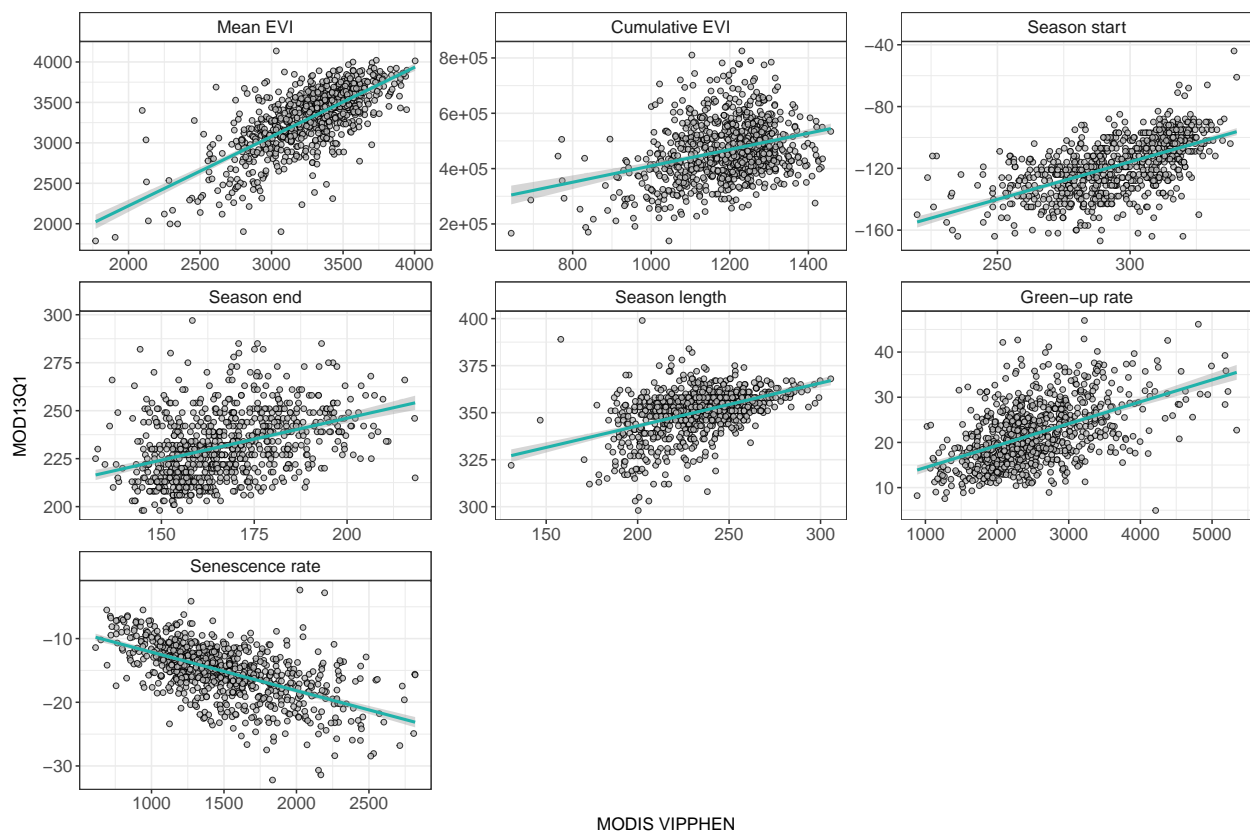


Figure S1

Response	DoF	F	Prob.	R ²
Mean EVI	809	845.6	p<0.05	0.51
Cumulative EVI	809	89.8	p<0.05	0.10
Season start	806	430.6	p<0.05	0.35
Season end	809	150.8	p<0.05	0.16
Season length	809	195.6	p<0.05	0.19
Green-up rate	809	281.2	p<0.05	0.26
Senescence rate	809	410.2	p<0.05	0.34

Table S1: Model fit statistics for comparison of MODIS VIPPHEN and MOD13Q1 products across each of our study sites.

Rank	Precipitation	Diurnal dT	Evenness	Richness	logLik	AIC	ΔIC	W_i
1	✓	✓	✓		-7843	15698	0.00	0.283
2	✓	✓			-7844	15699	0.65	0.205
3	✓	✓	✓	✓	-7842	15699	0.77	0.193
4	✓	✓		✓	-7843	15699	1.10	0.163
5	✓	✓	✓	✓	-7842	15701	2.56	0.079
6	✓	✓		✓	-7843	15701	2.63	0.076
7		✓	✓		-7851	15713	14.66	0.000
8		✓			-7852	15713	14.91	0.000
9		✓	✓	✓	-7851	15715	16.54	0.000
10		✓		✓	-7852	15715	16.87	0.000

Table S2: Cumulative EVI model selection candidate models, with fit statistics.

Rank	Precipitation	Diurnal dT	Evenness	Richness	logLik	AIC	ΔIC	W_i
1	✓	✓		✓	-2584	5180	0.00	0.272
2	✓	✓	✓	✓	-2583	5180	0.13	0.255
3		✓		✓	-2586	5182	1.93	0.104
4	✓	✓		✓	-2584	5182	1.99	0.101
5	✓	✓	✓	✓	-2583	5182	2.02	0.099
6		✓	✓	✓	-2585	5182	2.10	0.095
7		✓		✓	-2586	5184	3.93	0.038
8		✓	✓	✓	-2585	5184	4.05	0.036
9	✓			✓	-2595	5201	21.57	0.000
10	✓		✓	✓	-2595	5202	22.34	0.000

Table S3: Senescence lag model selection candidate models, with fit statistics.

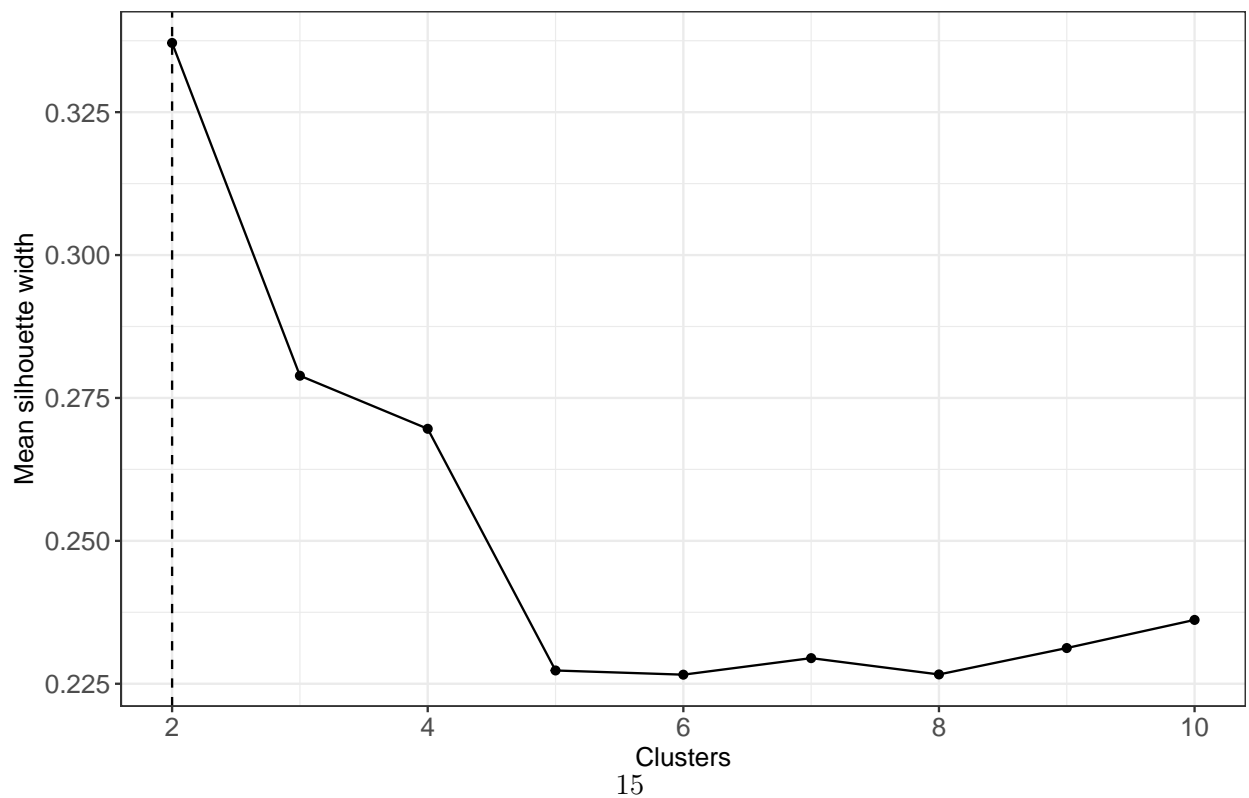


Figure S2

Rank	Precipitation	Diurnal dT	Evenness	Richness	logLik	AIC	ΔIC	W_i
1		✓		✓	-1987	3984	0.00	0.184
2	✓	✓		✓	-1986	3985	0.86	0.120
3		✓			-1988	3985	1.04	0.109
4		✓	✓	✓	-1986	3985	1.10	0.107
5	✓	✓			-1988	3986	1.53	0.086
6	✓	✓	✓	✓	-1986	3986	1.81	0.075
7		✓	✓		-1988	3986	1.83	0.074
8		✓		✓	-1987	3986	1.96	0.069
9	✓	✓	✓		-1987	3986	2.15	0.063
10	✓	✓		✓	-1986	3987	2.79	0.046

Table S4: Green-up rate model selection candidate models, with fit statistics.

Rank	Precipitation	Diurnal dT	Evenness	Richness	logLik	AIC	ΔIC	W_i
1	✓		✓	✓	-2226	4465	0.00	0.389
2	✓		✓	✓	-2226	4467	1.62	0.173
3	✓		✓		-2228	4467	1.75	0.162
4	✓	✓	✓	✓	-2226	4467	1.98	0.145
5	✓	✓	✓	✓	-2226	4469	3.57	0.065
6	✓	✓	✓		-2228	4469	3.62	0.064
7	✓			✓	-2234	4478	12.54	0.001
8	✓				-2235	4478	13.01	0.001
9	✓			✓	-2233	4478	13.08	0.001
10	✓	✓		✓	-2234	4480	14.54	0.000

Table S5: Season length model selection candidate models, with fit statistics.

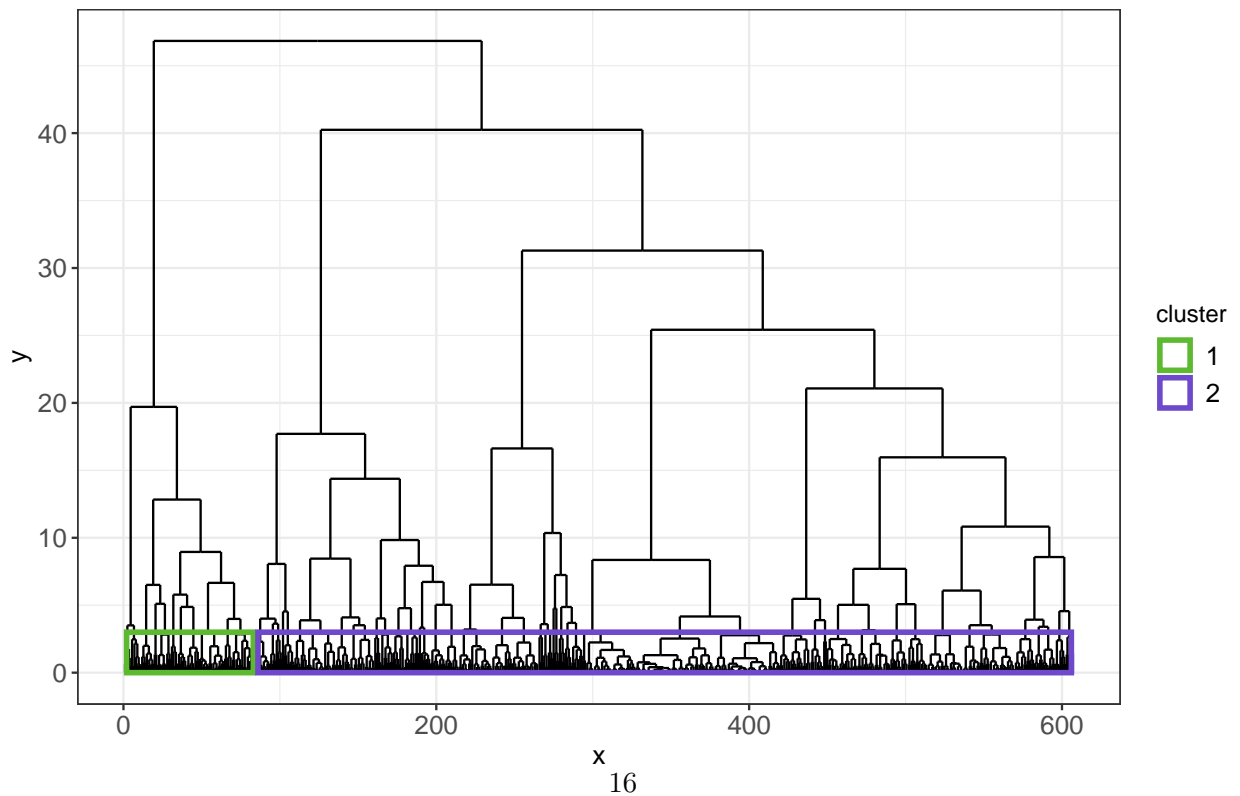


Figure S3

Rank	Precipitation	Diurnal dT	Evenness	Richness	logLik	AIC	ΔIC	W_i
1	✓	✓		✓	-1672	3357	0.00	0.248
2	✓	✓	✓	✓	-1672	3358	0.67	0.177
3	✓			✓	-1674	3359	1.74	0.104
4	✓	✓		✓	-1672	3359	2.00	0.091
5	✓		✓	✓	-1673	3359	2.21	0.082
6	✓	✓	✓	✓	-1672	3360	2.65	0.066
7	✓	✓			-1675	3360	3.00	0.055
8	✓				-1676	3360	3.36	0.046
9	✓			✓	-1674	3361	3.68	0.039
10	✓	✓	✓		-1674	3361	4.09	0.032

Table S6: Senescence rate model selection candidate models, with fit statistics.

Rank	Precipitation	Diurnal dT	Evenness	Richness	logLik	AIC	ΔIC	W_i
1	✓	✓		✓	-2516	5045	0.00	0.500
2	✓	✓	✓	✓	-2516	5047	1.60	0.224
3	✓	✓		✓	-2516	5047	1.91	0.192
4	✓	✓	✓	✓	-2516	5049	3.56	0.084
5	✓	✓			-2533	5077	31.54	0.000
6	✓	✓	✓		-2533	5079	33.53	0.000
7		✓		✓	-2554	5119	73.58	0.000
8		✓	✓	✓	-2553	5119	74.29	0.000
9		✓		✓	-2554	5120	75.06	0.000
10		✓	✓	✓	-2553	5121	75.98	0.000

Table S7: Green-up lag model selection candidate models, with fit statistics.